

A posteriori error analysis for a space-time parallel discretization of parabolic partial differential equations

Jehanzeb H. Chaudhry¹, Don Estep², and Simon Tavener³

¹Department of Mathematics and Statistics, University of New Mexico. Email: jehanzeb@unm.edu

²Department of Statistics and Actuarial Science, Simon Fraser University. Email: tavener@math.colostate.edu

³Department of Mathematics, Colorado State University. Email: donald_estep@sfu.ca

January 17, 2022

Abstract

We construct a space-time parallel method for solving parabolic partial differential equations by coupling the Parareal algorithm in time with overlapping domain decomposition in space. The goal is to obtain a discretization consisting of “local” problems that can be solved on parallel computers efficiently. However, this introduces significant sources of error that must be evaluated. Reformulating the original Parareal algorithm as a variational method and implementing a finite element discretization in space enables an adjoint-based *a posteriori* error analysis to be performed. Through an appropriate choice of adjoint problems and residuals the error analysis distinguishes between errors arising due to the temporal and spatial discretizations, as well as between the errors arising due to incomplete Parareal iterations and incomplete iterations of the domain decomposition solver. We first develop an error analysis for the Parareal method applied to parabolic partial differential equations, and then refine this analysis to the case where the associated spatial problems are solved using overlapping domain decomposition. These constitute our Time Parallel Algorithm (TPA) and Space-Time Parallel Algorithm (STPA) respectively. Numerical experiments demonstrate the accuracy of the estimator for both algorithms and the iterations between distinct components of the error.

Keywords — A posteriori error analysis, adjoint based error estimation, parabolic partial differential equations, Parareal, domain decomposition, Schwarz algorithms, time-parallel.

1 Introduction

Parallel computing approaches for solving complex problems modeled by partial differential equations have become increasingly attractive over the last decade, as Moore’s Law has continued, but transitioned from fabricating more transistors on a chip to constructing more cores. Spatial parallelization of partial differential equations is well established [3, 13, 32, 33, 41], but the improvement available through spatial parallelization alone typically decays as the number of processors increases for any fixed-size problem (the so-called strong scaling behavior), see e.g., [20]. Parallel in time methods provide an additional way to effectively utilize modern high performance computer architectures [15, 19, 22, 28, 29, 35, 38]. Unfortunately parallel-in-time methods also introduce significant additional sources of error which must be estimated for the purposes of validation when seeking to construct adaptive algorithms, or when performing uncertainty quantification.

We consider a PDE system of the form: Find $u(x, t) \in L^2(0, T; H_0^1(\Omega))$ such that

$$\begin{aligned} (\dot{u}, v) + a(u, v) &= l(v), \quad \forall v \in H_0^1(\Omega) \text{ and } t \in (0, T], \\ u(x, 0) &= u_0(x), \end{aligned} \tag{1}$$

where $\dot{u} = \frac{\partial u}{\partial t}$, $a(\cdot, \cdot)$ is a coercive, positive definite bilinear form, $l(\cdot)$ is a linear form, Ω is a convex polygonal domain, and $u_0 \in H_0^1$ is the initial condition. Here (\cdot, \cdot) denotes the $L_2(\Omega)$ inner product, so that $(w, v) = \int_{\Omega} wv \, dx$. We assume that the forms a and l satisfy sufficient regularity assumptions so that a weak solution $u(x, t) \in L^2(0, T; H_0^1(\Omega))$ exists and is unique [31]. Further, we consider a quantity of interest (QoI) given by

$$\mathcal{Q}(u) = \int_{\Omega} \psi(x)u(x, T) \, dx \tag{2}$$

where $\psi \in L^2(\Omega)$.

The aim of this work is to derive error estimates for the numerically computed value of \mathcal{Q} when time-parallel and spatial domain decomposition techniques are employed for the approximation of $u(x, t)$. In particular, we consider two algorithms which we call the Time Parallel Algorithm (TPA) and the Space-Time Parallel Algorithm (STPA). The TPA implements the Parareal algorithm [14, 21, 26, 34, 36], a time-parallel method to solve (1), while the STPA also employs a parallel domain decomposition strategy in space [30, 37, 39, 40] in addition to the time-parallelism of the Parareal method.

The analysis presented here extends earlier work on the *a posteriori* error analysis of the Parareal algorithm in [7], and incorporates the work of [4] on the *a posteriori* error analysis of overlapping Schwarz domain decomposition algorithms to provide an estimate of the spatial discretization error. One significant difference between the earlier work and the current work is that we analyze the effects of using an iterative method to solve the discrete equations arising from an implicit time integration scheme. The analysis builds on early work of adjoint-based *a posteriori* error analysis [1, 2, 17, 27] and more recent work addressing iterative and multi-rate methods [6, 10, 18].

1.1 Notation

Our analysis requires consideration of both exact and discrete solutions. Analytical solutions are indicated using a lower case letter, discrete solutions with an upper case letter. Solutions of the PDE will be designated u and adjoint solutions ϕ . A hat indicates a coarse scale entity. Errors are indicated using e and residuals with \mathcal{R} . A dot indicates a partial differential in time. We use N to indicate the number of finite elements, Q to indicate the degree of interpolation, P to indicate the number of temporal or spatial subdomains, and K to indicate the number of iterations. A subscript t for these symbols indicates a temporal quantity, a subscript s indicates a spatial quantity. A full list of variables and discretization choices appears in A.

For a function $w(x, t)$, we denote $w(t) := w(\cdot, t)$, i.e., $w(t)$ refers to a function of space only for a fixed time t . We use the notation $(w, v)(t) := (w(t), v(t)) = \int_{\Omega} w(x, t)v(x, t) \, dx$, so for example the QoI (2) may be expressed as $\mathcal{Q}(u) = (\psi, u)(T)$. Finally, we let $\langle \cdot \rangle_I$ indicate integration over time interval I , i.e. $\langle \cdot \rangle_I = \int_I \cdot \, dt$.

1.2 Outline

We begin the analysis from the perspective of Parareal integration in time, presented in [7]. The Parareal approach utilizes both coarse and fine scale discretizations in time. Extending this analysis to PDEs requires corresponding coarse and fine discretizations in space. Since we implement a domain decomposition strategy in space, we employ iterative solution methods in both time and space.

We introduce two algorithms in section 2: a Time Parallel Algorithm (TPA), and a Space-Time Parallel Algorithm (SPTA). The TPA employs the time-parallel algorithm, Parareal, for the solution of PDEs, whereas the SPTA additionally utilizes additive Schwarz domain decomposition to achieve parallelization

in space. This section also contains precise details of the spatial and temporal discretizations. We recall some essential mathematical results needed for the subsequent analysis for the two algorithms in section 3. We adjust the previous *a posteriori* error analysis for Parareal time integration to analyze the TPA in section 4. We extend this analysis to account for the errors arising using additive Schwarz domain decomposition in section 5. Numerical results supporting the accuracy of the *a posteriori* error estimates are provided in section 6.

2 Discretizations: The “Time Parallel Algorithm” and the “Space-Time Parallel Algorithm”

We consider two algorithms: (1) An algorithm which is parallel in time only, referred to as Time Parallel Algorithm (TPA), and (2) An algorithm which is parallel in both space and time, referred to as Space-Time Parallel Algorithm (STPA). Both algorithms use the Parareal algorithm for time-parallelism. The spatial parallelization in STPA is achieved through the use of overlapping Schwarz domain decomposition method. The discretization also involves using the finite element method in space and the implicit Euler method in time. The implicit Euler method is appropriate for dissipative problems modeled by (1). We describe these algorithms in detail below.

2.1 Time Parallel Algorithm (TPA)

The Parareal algorithm is based on a pair of coarse and fine scale solvers, $\widehat{G}^p[\alpha(x)](t)$ and $F^p[\alpha(x)](t)$ respectively. Let $0 = T_0 < \dots < T_{p-1} < T_p < \dots < T_P = T$ be a partition of the time domain. We view the times T_p as “synchronization” times at which point the coarse and fine scale solutions may exchange information. We call the time interval $[T_{p-1}, T_p]$ the temporal subdomain p , see Figure 1. Note that the temporal subdomains are non-overlapping.

The numerical solver $F^p[\alpha(x)](t)$ is more accurate than $\widehat{G}^p[\alpha(x)](t)$, e.g., employing a finer discretization or a higher order method. The super-script p indicates that the solvers produce a space-time solution for the temporal subdomain p . That is, for $t \in (T_{p-1}, T_p]$, $\widehat{G}^p[\alpha(x)](t)$ (resp. $F^p[\alpha(x)](t)$) indicates the space-time coarse scale (resp. fine scale) solution at t , where $\alpha(x)$ denotes the initial conditions for the solver at $t = T_{p-1}$. Specific examples of the solvers are presented in 2.1.1.

The standard version of the Parareal algorithm defines the solutions only at the times T_p and is not amenable to adjoint-based *a posteriori* analysis, which requires solutions to be in variational form. An equivalent, variational version of the Parareal algorithm, suitable for an adjoint-based *a posteriori* error analysis, is provided in Algorithm 1. The standard Parareal algorithm is provided in B and a proof of its equivalence with the variational version is given in [7]. Here $\widehat{U}^{p, \{k_t\}}(x, t)$ and $U^{p, \{k_t\}}(x, t)$ are the coarse and fine scale solutions for the variational Parareal algorithm at iteration k_t on temporal subdomain p . The fine-scale Parareal solution after k_t iterations is defined to be $U^{\{k_t\}} = U^{p, \{k_t\}}$ for $t \in (T_{p-1}, T_p]$. The initial condition approximation to u_0 is referred to as \widehat{U}_0 . Note that since \widehat{U}_0 is represented in a finite dimensional space, it is possible that $u_0 \neq \widehat{U}_0$.

Algorithm 1 Variational form of the Parareal algorithm

```

procedure VPAR( $P_t, K_t, \widehat{U}_0$ )
     $C^{p,\{0\}} = 0, p = 0, \dots, P_t$  ▷ Initialize corrections
    for  $k_t = 1, \dots, K_t$  do
         $\widehat{U}^{0,\{k_t\}}(x, 0) := \widehat{U}_0$  ▷ Set initial conditions
        for  $p = 1, \dots, P_t$  do
             $\widehat{U}^{p,\{k_t\}}(x, t) = \widehat{G}^p[\widehat{U}^{p-1,\{k_t\}}(x, T_{p-1}) + C^{p,\{k_t-1\}}(x)](t)$  ▷ Serial computation
             $U^{p,\{k_t\}}(x, t) = F^p[\widehat{U}^{p,\{k_t\}}(x, T_{p-1})](t)$  ▷ Parallel computation
             $C^{p,\{k_t\}}(x) = U^{p,\{k_t\}}(x, T_p) - \widehat{G}^p[\widehat{U}^{p,\{k_t\}}(x, T_{p-1})](T_p)$  ▷ Update corrections
        end for
    end for
    return  $U^{p,\{K_t\}}(x, t)$ 
end procedure
    
```

2.1.1 Temporal and spatial discretizations of the fine scale and coarse scale solvers

We consider the implicit Euler method for time discretization and finite elements for the spatial discretization to define coarse and fine scale solutions on $[T_{p-1}, T_p]$. We omit the superscript p in this section when the temporal subdomain is clear.

We discretize the **spatial** domain Ω into a quasi-uniform triangulation \mathcal{T}_h , where h denotes the maximum diameter of the elements. This triangulation is chosen so the union of the elements of \mathcal{T}_h is Ω and the intersection of any two elements is either a common edge, node, or is empty. Let V_s^q be the standard space of continuous piecewise polynomials of degree q on \mathcal{T}_h , such that if $U \in V_s^q$ then $U = 0$ on $\partial\Omega$. In particular, we consider a coarse space $V_s^{\widehat{q}_s}$ and fine space $V_s^{q_s}$ such that $\widehat{q}_s < q_s$.

On each **time** subdomain p , the coarse temporal discretization, uses \widehat{N}_t^p time steps while the fine temporal discretization uses N_t^p time steps. Thus, the total coarse time steps over $[0, T]$ are $\widehat{N}_t = \sum_{p=1}^{P_t} \widehat{N}_t^p$, and the total fine time steps are $N_t = \sum_{p=1}^{P_t} N_t^p$. On the coarse scale, we partition $[T_{p-1}, T_p]$ as $T_{p-1} = \widehat{t}_0^p < \dots < \widehat{t}_{\widehat{N}_t^p-1}^p < \widehat{t}_{\widehat{N}_t^p}^p = T_p$, as shown in Figure 1, with $\widehat{\mathcal{I}}_{\widehat{n}}^p = [\widehat{t}_{\widehat{n}-1}^p, \widehat{t}_{\widehat{n}}^p]$. Let $\widehat{\mathcal{T}}^p = \{\widehat{\mathcal{I}}_1^p, \dots, \widehat{\mathcal{I}}_{\widehat{n}}^p, \dots, \widehat{\mathcal{I}}_{\widehat{N}_t^p}^p\}$. On the fine scale we introduce a finer discretization $T_{p-1} = t_0^p < \dots < t_{N_t^p-1}^p < t_{N_t^p}^p = T_p$ as shown in Figure 1. We let $\mathcal{I}_{\widehat{n}}^p = [t_{\widehat{n}-1}^p, t_{\widehat{n}}^p]$ and $\mathcal{T}^p = \{\mathcal{I}_1^p, \dots, \mathcal{I}_{\widehat{n}}^p, \dots, \mathcal{I}_{N_t^p}^p\}$.

We now use the implicit Euler method on the coarse time step $\widehat{\mathcal{I}}_{\widehat{n}}^p$: given the approximate solution \widehat{U}_{n-1} at $\widehat{t}_{\widehat{n}-1}^p$, compute approximation $\widehat{U}_n \in V_s^{\widehat{q}_s}$ at $\widehat{t}_{\widehat{n}}^p$ by,

$$(\widehat{U}_n, v) = (\widehat{U}_{n-1}, v) + \Delta \widehat{t}_{\widehat{n}}^p \left[-a(\widehat{U}_n, v) + l(v) \right], \quad (3)$$

for all $v \in V_s^{\widehat{q}_s}$, where $\Delta \widehat{t}_{\widehat{n}}^p = (\widehat{t}_{\widehat{n}}^p - \widehat{t}_{\widehat{n}-1}^p)$. Moreover, in the context of Parareal algorithm, we have $\widehat{U}_{n-1} \in V_s^{\widehat{q}_s}$ for all \widehat{n} except possibly for $\widehat{n} = 1$, where \widehat{U}_0 (the initial condition for the coarse scale solver) may belong to V_s^q .

Similarly, the implicit Euler method on the fine time step $\mathcal{I}_{\widehat{n}}^p$ is: given the approximate solution U_{n-1} at $t_{\widehat{n}-1}^p$, compute approximation $U_n \in V_s^q$ at $t_{\widehat{n}}^p$ by,

$$(U_n, v) = (U_{n-1}, v) + \Delta t_{\widehat{n}}^p \left[-a(U_n, v) + l(v) \right], \quad (4)$$

for all $v \in V_s^q$, where $\Delta t_{\widehat{n}}^p = (t_{\widehat{n}}^p - t_{\widehat{n}-1}^p)$. In the context of Parareal algorithm, we have $U_{n-1} \in V_s^q$ for all n except for $n = 1$ for which U_0 (the initial condition for the fine scale solver) belongs to $V_s^{\widehat{q}_s}$.

In the TPA, we assume that equations 3 and 4 are solved exactly (up to numerical precision).

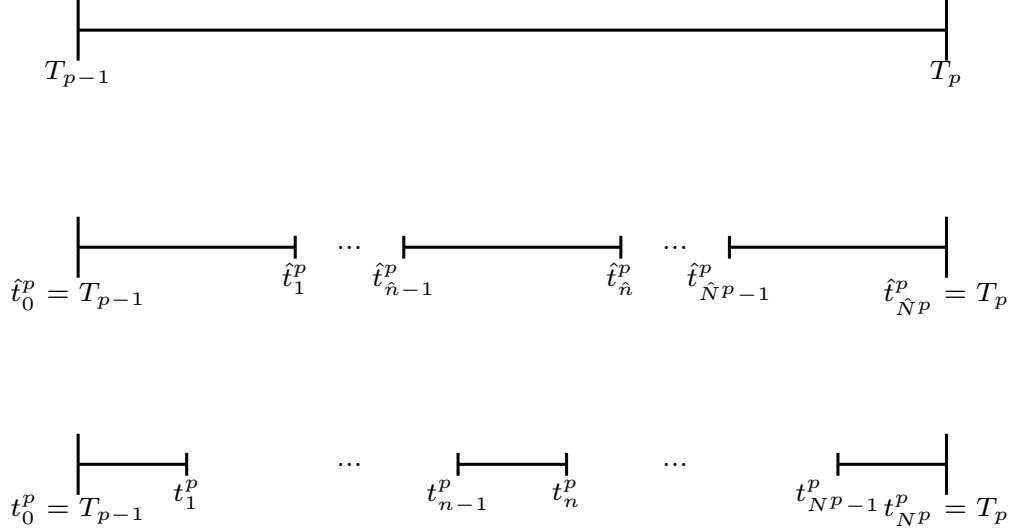


Figure 1: Top: Subdomain $[T_{p-1}, T_p]$. Middle: Stage 1 discretization for $[T_{p-1}, T_p]$. Bottom: Stage 2 discretization for $[T_{p-1}, T_p]$.

2.2 Space-Time Parallel Algorithm (STPA)

The STPA introduces spatial parallelization (in addition to temporal parallelization) by using a Schwarz domain decomposition iteration at the fine scale. It is assumed in the spirit of the Parareal algorithm that the coarse scale is solved implicitly without needing any spatial domain decomposition.

2.2.1 Schwarz Domain Decomposition at a single time step

The additive Schwarz Domain decomposition iteration is employed to solve the spatial problem in (4). Similar to §2.1.1, we omit the subscript p where this is clear. We rewrite the problem (4) on subinterval \mathcal{I}_n^p as: find $U_n \in V_s^{q_s}$ such that,

$$B^n(U_n, v) = l^n(v) \quad (5)$$

for all $v \in V_s^q$, where the bilinear form $B^n(\cdot, \cdot)$ and the linear form $l^n(\cdot)$ are defined by,

$$\begin{aligned} B^n(u, v) &= (u, v) + \Delta t_n^p a(u, v), \\ l^n(v) &= (U_{n-1}, v) + \Delta t_n^p l(v). \end{aligned} \quad (6)$$

Assume that we have P_s overlapping subdomains $\Omega_1, \dots, \Omega_{P_s}$ on Ω , such that for any Ω_i , there exists a Ω_j , $i \neq j$, for which $\Omega_i \cap \Omega_j \neq \emptyset$ and $\cup_i \Omega_i = \Omega$. Let $\mathcal{T}_{h,i} \equiv \mathcal{T}_h \cap \Omega_i$. We further assume that the triangulation \mathcal{T}_h is consistent with the domain decomposition in the sense that for any $T_s \in \mathcal{T}_h$, if $T_s \cap \Omega_j \neq \emptyset$ then $T_s \subset \Omega_j$. We let $(\cdot, \cdot)_{ij}$ represent the $L_2(\Omega_i \cap \Omega_j)$ inner product. We denote by $B_i^n(\cdot, \cdot)$ the restriction of $B^n(\cdot, \cdot)$ to Ω_i and $B_{ij}^n(\cdot, \cdot)$ the restriction of $B^n(\cdot, \cdot)$ to $\Omega_i \cap \Omega_j$. Similarly, we let $l_i^n(\cdot)$ be the restriction of $l^n(\cdot)$ to Ω_i . The additive Schwarz method for the solution of (5) is given in Algorithm 2. The domain decomposition solution for $n = 1, \dots, N_t^p$ are $U_n^{\{K_s\}} = \text{ASDD}(B^n, l^n, K_s, P_s, U_{n-1}^{\{K_s\}})$. Note that the initial guess to the algorithm is the solution from the previous time step $U_{n-1}^{\{K_s\}}$. In the algorithm $V_i^{q_s}$ represents the space of continuous piecewise polynomials of degree q_s on $\mathcal{T}_{h,i}$ such that if $U \in V_i^{q_s}$ then $U = 0$ on $\partial\Omega_i$, and $V_{i,k_s}^{q_s}$ represents the space of continuous piecewise polynomials of degree q_s on $\mathcal{T}_{h,i}$ such that if $U \in V_{i,k_s}^{q_s}$ then $U = 0$ on $\partial\Omega$ and $U = U_n^{\{k_s\}}$ on $\partial\Omega_i \setminus \partial\Omega$. The Richardson parameter τ , is needed to ensure that the iteration converges [37].

Algorithm 2 Overlapping additive Schwarz domain decomposition

```

procedure ASDD( $B^n, l^n, K_s, P_s, U_n^{\{0\}}$ )
  for  $k = 0, 1, 2, \dots, K_s - 1$  do
    for  $i = 1, 2, \dots, P_s$  do
      Find  $\tilde{U}_{n,i}^{\{k_s+1\}} \in V_{i,k_s}^{q_s}$  such that
    
```

$$B_i^n(\tilde{U}_{n,i}^{\{k_s+1\}}, v) = l_i^n(v), \quad \forall v \in V_i^{q_s}. \quad (7)$$

Let

$$U_n^{\{k_s+1\}} = (1 - \tau P_s)U_n^{\{k_s\}} + \tau \left(\sum_{i=1}^{P_s} \Pi_i \tilde{U}_{n,i}^{\{k_s+1\}} \right) \quad \text{where} \quad \Pi_i \tilde{U}_{n,i}^{\{k_s+1\}} = \begin{cases} \tilde{U}_{n,i}^{\{k_s+1\}}, & \text{on } \bar{\Omega}_i, \\ U_n^{\{k_s\}}, & \text{on } \Omega \setminus \bar{\Omega}_i. \end{cases} \quad (8)$$

```

    end for
  end for
  return  $U_n^{\{K_s\}}$ 
end procedure

```

2.2.2 The global STPA solution

In the context of the Parareal algorithm (Algorithm 1), we denote the solution by $U^{p,\{k_t, K_s\}}$, where we have now added K_s to the superscript to indicate the dependence of the solution on domain decomposition iterations at the k_t th Parareal iteration. The global STPA solution on $[0, T]$ after k_t Parareal iterations and K_s domain decomposition iterations is defined as $U^{\{k_t, K_s\}} = U^{p,\{k_t, K_s\}}$ for $t \in (T_{p-1}, T_p]$.

3 Variational methods and preliminary *a posteriori* error analysis

In this section, we introduce basic elements needed for the error analysis of the numerical value of the QoI (see (2)) computed using the fine scale solution from either the the Time Parallel Algorithm or the Space-Time Parallel Algorithm. The main tools used in the analysis are adjoint problems coupled with an appropriate definition of residuals. This kind of analysis relies on the solution being in a variational format. Hence, we present the implicit Euler method as a variational method in §3.3, and point out a fundamental property of variational methods which is used subsequently in the analysis of TPA and STPA.

3.1 Variational methods

We define two variational methods; the continuous Galerkin method and the discontinuous Galerkin method for the fine scale; the extension to the coarse scale is analogous. Note that the usage of “continuous” or “discontinuous” refers to the property of the solution in time only; in space we always use continuous finite elements.

On the space-time slab $S_n^p = \Omega \times \mathcal{I}_n^p$ we define the space

$$W_{p,n}^{q_t, q_s} := \{w(x, t) : w(x, t) = \sum_{j=0}^{\hat{q}_t} t^j v_j(x), v_j \in V_s^{q_s}, (x, t) \in S_n^p\}, \quad (9)$$

The **continuous Galerkin method**, $\mathbf{cG}(q_t)$ is: find U_{CG} such that it is continuous on S_n^p , its restriction to S_n^p belongs to $W_{p,n}^{q_t, q_s}$ and also satisfies,

$$\langle (\dot{U}_{CG}, v) \rangle_{\mathcal{I}_n^p} = \langle -a(U_{CG}, v) + l(v) \rangle_{\mathcal{I}_n^p} \quad (10)$$

for all $v \in W_{p,n}^{q_t-1, q_s}$.

We denote the jump across t_n^p as $[w]_{n,p} = w_{n,p}^+ - w_{n,p}^-$, where $w_{n,p}^\pm = \lim_{s \rightarrow (t_n^p)^\pm} w(s)$. The **discontinuous Galerkin method, dG(q_t)** is: find U_{CG} its restriction to S_n^p belongs to $W_{p,n}^{q_t, q_s}$ and also satisfies,

$$\langle (\dot{U}_{DG}, v) \rangle_{\mathcal{I}_n^p} + ([U_{DG}]_{n-1,p}, v_{n-1,p}^+) = \langle -a(U_{DG}, v) + l(v) \rangle_{\mathcal{I}_n^p} \quad (11)$$

for all $v \in W_{p,n}^{q_t, q_s}$. Note that the solution may be discontinuous in at the time nodes t_n^p .

3.2 A posteriori error analysis for variational methods on a single time subdomain

Variational methods satisfy an important property that underpins the *a posteriori* error analysis presented here. Let $\phi \in L^2(T_{p-1}, T_p; H_0^1(\Omega))$ satisfy,

$$(-\dot{\phi}, v) = -a(v, \phi) \quad \forall v \in H_0^1(\Omega) \text{ and } t \in (T_{p-1}, T_p] \quad (12)$$

Equation (12) is referred to as an adjoint equation. Next we quantify the accumulation of error contributions.

Lemma 1. *Let $e_{\text{Var}} = u - U_{\text{Var}}$, where u is the solution to (1), $\text{Var} \in \{CG, DG\}$ and U_{Var} is either the cG(q_t) or the dG(q_t) solution on a time subdomain p . Then,*

$$(\phi, e_{\text{Var}})(T_p) = (\phi, e_{\text{Var}})(T_{p-1}) + \mathcal{R}_{\text{Var}}^p(U_{\text{Var}}, \phi) \quad (13)$$

where ϕ is defined in (12) and $\mathcal{R}_{\text{Var}}^p(U_{\text{Var}}, \phi)$ is the adjoint-weighted space-time residual of the solution U_{Var} on time subdomain p defined as

$$\mathcal{R}_{\text{Var}}^p(U_{\text{Var}}, \phi) = \begin{cases} \sum_{n=1}^{N_p} \left[\langle l(v) - a(U_{CG}, v) \rangle_{\mathcal{I}_n^p} - \langle (\dot{U}_{CG}, v) \rangle_{\mathcal{I}_n^p} \right], & \text{if Var} = CG, \\ \sum_{n=1}^{N_p} \left[\langle l(v) - a(U_{DG}, v) \rangle_{\mathcal{I}_n^p} - \langle (\dot{U}_{DG}, v) \rangle_{\mathcal{I}_n^p} - ([U_{DG}]_{n-1,p}, \phi_{n-1,p}^+) \right], & \text{if Var} = DG. \end{cases} \quad (14)$$

Proof. We prove property (13) for the dG method, the proof for the cG method is similar. In the notation of the dG method, we have

$$e_{\text{Var}}(T_{p-1}) = e_{\text{Var}}^+(t_0^p) \quad \text{and} \quad e_{\text{Var}}(T_p) = e_{\text{Var}}^-(t_{N_p}^p). \quad (15)$$

Consider

$$\langle (-\dot{\phi}, e_{DG}) \rangle_{\mathcal{I}_n^p} = -\langle a(e_{DG}, \phi) \rangle_{\mathcal{I}_n^p}. \quad (16)$$

The left-hand side is

$$\langle (-\dot{\phi}, e_{DG}) \rangle_{\mathcal{I}_n^p} = -(\phi, e_{DG}^-)(t_n^p) + (\phi, e_{DG}^+)(t_{n-1}^p) + \langle (\phi, \dot{u} - \dot{U}_{DG}) \rangle_{\mathcal{I}_n^p}. \quad (17)$$

Combining (16) and (17) with (1) leads to

$$\begin{aligned} (\phi, e_{DG}^-)(t_n^p) &= (\phi, e_{DG}^+)(t_{n-1}^p) + \langle l(v) - a(U_{DG}^p, v) \rangle_{\mathcal{I}_n^p} - \langle (\dot{U}_{DG}, v) \rangle_{\mathcal{I}_n^p}, \\ &= (\phi, e_{DG}^-)(t_{n-1}^p) - (\phi_{n-1,p}^+, [U_{DG}]_{n,p}) + \langle l(v) - a(U_{DG}^p, v) \rangle_{\mathcal{I}_n^p} - \langle (\dot{U}_{DG}, v) \rangle_{\mathcal{I}_n^p} \end{aligned} \quad (18)$$

Summing (18) over $n = 1$ to $n = N_t^p$ and using (15),

$$(\phi, e_{DG})(T_p) = (\phi, e_{DG})(T_{p-1}) + \mathcal{R}^p(U_{DG}, \phi), \quad (19)$$

which is the desired result. \square

Note that a similar result, with similar derivation, also holds for the coarse scale.

3.3 *A posteriori* error analysis for implicit Euler on a single time subdomain

It is well known that the implicit Euler method with a certain choice of quadrature is nodally equivalent to the $dG(0)$ method and hence may be considered a variational method [16]. For completeness, we show this equivalence for the $dG(0)$ in (11) with the implicit Euler method in (4). For the $dG(0)$ method, we have $\dot{U}_{DG} = 0$, since the solution is constant in time over \mathcal{I}_n^p for a fixed spatial point. Moreover, $W_{p,n}^{0,q_s}$ is simply $V_s^{q_s}$. Now, using these facts, along with the right-hand rule of evaluating quadrature in (11),

$$((U_{DG})_{n,p}^- - (U_{DG})_{n,p}^+, v_{n-1,p}^+) = \Delta t_n^p [a((U_{DG})_{n,p}^-, v_{n,p}^-) + l(v)] \quad (20)$$

Now, since $v \in W_{p,n}^{0,q_s}$ is constant in time, we have $v_{n-1,p}^+ = v_{n,p}^- = v$. Finally, identifying $(U_{DG})_{n,p}^-$ with U_n and $(U_{DG})_{n,p}^+$ with U_{n-1} completes the equivalence of the two equations.

Now we define coarse and fine scale analogues to (14) for the implicit Euler method. The fine scale residuals are,

$$\mathcal{R}_n^p(w, v) = \langle l(v) - a(w, v) \rangle_{\mathcal{I}_n^p} - ([w]_{n-1,p}, v^+), \quad (21)$$

$$\mathcal{R}^p(w, v) = \sum_{n=1}^{N_p} \mathcal{R}_n^p(w, v). \quad (22)$$

The coarse scale residuals are,

$$\widehat{\mathcal{R}}_n^p(w, v) = \langle l(v) - a(w, v) \rangle_{\widehat{\mathcal{I}}_n^p} - ([w]_{\widehat{n}-1,p}, v^+), \quad (23)$$

$$\widehat{\mathcal{R}}^p(w, v) = \sum_{\widehat{n}=1}^{\widehat{N}_p} \widehat{\mathcal{R}}_n^p(w, v). \quad (24)$$

Notice that there is no time derivative in the residuals because, as discussed earlier, those terms are 0 for the $dG(0)$ method.

The analogues of property (13) for the coarse and fine scale solutions in Algorithm 1 follow immediately. Let $U^p = F^p[U^p(T_{p-1})]$ be the fine-scale solution on time domain p , and $e^p = u - U^p$. Then,

$$(\phi, e^p)(T_p) = (\phi, e^p)(T_{p-1}) + \mathcal{R}^p(U^p, \phi). \quad (25)$$

Let $\widehat{U}^p = \widehat{G}[\widehat{U}^p(T_{p-1})]$ be the coarse scale solution on time domain p . Let $\widehat{e}^p = u - \widehat{U}^p$. Then,

$$(\phi, \widehat{e}^p)(T_p) = (\phi, \widehat{e}^p)(T_{p-1}) + \widehat{\mathcal{R}}^p(\widehat{U}^p, \phi). \quad (26)$$

4 *A posteriori* error analysis for the Time Parallel Algorithm (TPA)

In this section we derive estimates for the error in the QoI computed from the fine scale solution of the TPA presented in §2.1. That is, we seek to estimate $\mathcal{Q}(u - U^{\{K_i\}}) = (\psi, u(T) - U^{\{K_i\}}(T))$. The analysis for TPA is quite similar to the analysis for ODEs appearing in [7], except that the analysis for PDEs includes the error in the initial conditions, which is assumed to be zero for ODEs.

4.1 Coarse and fine scale adjoint problems

The coarse scale adjoint problem is: find $\widehat{\phi} \in L^2(0, T; H_0^1(\Omega))$ such that

$$\left. \begin{aligned} (-\dot{\widehat{\phi}}, v) &= -a(v, \widehat{\phi}) \quad \forall v \in H_0^1(\Omega) \text{ and } t \in (0, T], \\ \widehat{\phi}(T) &= \psi. \end{aligned} \right\} \quad (27)$$

Here, the term ‘‘coarse’’ indicates that in numerical experiments, this adjoint is approximated using a coarse (spatial and temporal) scale space.

For $p = 1, 2, \dots, P_t$, the fine scale adjoint problem for the p th time domain $[T_{p-1}, T_p]$ is: find $\phi^p \in L^2(T_{p-1}, T_p; H_0^1(\Omega))$ such that

$$\left. \begin{aligned} (-\dot{\phi}^p, v) &= -a(v, \phi^p) \quad \forall v \in H_0^1(\Omega) \text{ and } t \in (T_{p-1}, T_p], \\ \phi^p(T_p) &= \widehat{\phi}(T_p). \end{aligned} \right\} \quad (28)$$

Notice that the fine scale adjoint problem on the p th time subdomain receives initial conditions from the coarse scale adjoint problem and therefore the adjoint on the fine temporal scale can be solved independently on each of the p time domains. However, while reducing solution cost, the resulting discontinuities in the fine temporal scale adjoint solution occurring at the boundaries of temporal subdomains give rise to an additional contribution to the error. In numerical experiments, the fine scale adjoints are approximated using a fine (relative to the space used for the approximation of the coarse scale adjoints) scale space.

We seek the error in the fine scale solution below. However, since coarse scale solutions are used as initial conditions for fine scale integration on each subdomain, the analysis indicates the expected interaction between errors at the two different scales.

4.2 Error representations

Let $e^{\{k_t\}} = u - U^{\{k_t\}}$ and $\widehat{e}^{\{k_t\}} = u - \widehat{U}^{\{k_t\}}$.

Lemma 2.

$$\begin{aligned} (\psi, e^{\{k_t\}}(T)) &= \sum_{p=1}^{P_t} \mathcal{R}^p(U^{p, \{k_t\}}, \phi^p) + (\phi^1, \widehat{e}^{1, \{k_t\}})(0) \\ &\quad + \sum_{p=2}^{P_t} \left[(\phi^p - \widehat{\phi}, \widehat{e}^{p-1, \{k_t\}}) + (\phi^p - \widehat{\phi}, \widehat{U}^{p-1, \{k_t\}} - \widehat{U}^{p, \{k_t\}}) + (\widehat{\phi}, U^{p-1, \{k_t\}} - U^{p, \{k_t\}}) \right] (T_{p-1}). \end{aligned} \quad (29)$$

Proof. By definition of $U^{\{k_t\}}$, we have $U^{\{k_t\}}(T) = U^{P_t, \{k_t\}}(T) = U^{P_t, \{k_t\}}(T_{P_t})$. From (25) and $\phi^p(T_p) = \widehat{\phi}(T_p)$ (see (28)) we have

$$(\widehat{\phi}, e^{p, \{k_t\}})(T_p) = (\phi^p, e^{p, \{k_t\}})(T_{p-1}) + \mathcal{R}^p(U^{p, \{k_t\}}, \phi^p). \quad (30)$$

Summing over all time subdomains from $p = 1$ to P_t , and isolating $(\psi, e^{P_t, \{k_t\}}(T)) = (\psi, e^{\{k_t\}}(T))$ leads to

$$(\psi, e^{\{k_t\}}(T)) = - \sum_{p=1}^{P_t-1} (\widehat{\phi}, e^{p, \{k_t\}})(T_p) + \sum_{p=2}^{P_t} (\phi^p, e^{p, \{k_t\}})(T_{p-1}) + \sum_{p=1}^{P_t} \mathcal{R}^p(U^{p, \{k_t\}}, \phi^p) + (\phi^1, e^{1, \{k_t\}})(0). \quad (31)$$

Using $U^{p, \{k_t\}}(T_{p-1}) = \widehat{U}^{p, \{k_t\}}(T_{p-1})$ (see Algorithm 1),

$$(\psi, e^{\{k_t\}}(T)) = - \sum_{p=1}^{P_t-1} (\widehat{\phi}, e^{p, \{k_t\}})(T_p) + \sum_{p=2}^{P_t} (\phi^p, \widehat{e}^{p, \{k_t\}})(T_{p-1}) + \sum_{p=1}^{P_t} \mathcal{R}^p(U^{p, \{k_t\}}, \phi^p) + (\phi^1, \widehat{e}^{1, \{k_t\}})(0). \quad (32)$$

Rearranging, adding and subtracting terms as necessary, we arrive at

$$\begin{aligned}
 (\psi, e^{\{k_t\}}(T)) &= \sum_{p=1}^{P_t} \mathcal{R}^p(U^{p,\{k_t\}}, \phi^p) + (\phi^1, \widehat{e}^1)(0) \\
 &+ \sum_{p=2}^{P_t} \left[(\phi^p - \widehat{\phi}, \widehat{e}^{p-1,\{k_t\}}) + (\phi^p - \widehat{\phi}, \widehat{U}^{p-1,\{k_t\}} - \widehat{U}^{p,\{k_t\}}) + (\widehat{\phi}, U^{p-1,\{k_t\}} - U^{p,\{k_t\}}) \right] (T_{p-1}).
 \end{aligned} \tag{33}$$

□

The terms $(\phi^p - \widehat{\phi}, \widehat{e}^{p-1,\{k_t\}})(T_{p-1})$ in the error representation (29) are not directly computable as they contain the unknown error \widehat{e}^{p-1} . We solve auxiliary adjoint problems to account for these error terms. As noted earlier, this is the tradeoff between solving the fine-scale adjoint problem from T to 0 and solving P adjoint problems on each subdomain independently using the coarse scale adjoint problem as “initial” conditions. Consider $(P_t - 1)$ auxiliary (coarse scale) QoIs as

$$\Psi(u) = (\phi^p - \widehat{\phi}, u), \tag{34}$$

and $(P_t - 1)$ auxiliary adjoint problems: find $\widehat{\phi}_{\text{aux}}^p \in L^2(0, T_{p-1}; H_0^1(\Omega))$ such that

$$\left. \begin{aligned}
 -\dot{\widehat{\phi}}_{\text{aux}}^p &= -a(v, \widehat{\phi}_{\text{aux}}^p), \quad \forall v \in H_0^1(\Omega) \text{ and } t \in (0, T_{p-1}] \\
 \widehat{\phi}_{\text{aux}}^p(x, T_{p-1}) &= \phi^p(x, T_{p-1}) - \widehat{\phi}(x, T_{p-1}).
 \end{aligned} \right\} \tag{35}$$

Replacing ϕ by $\widehat{\phi}_{\text{aux}}^p$ in (26) on k th time subdomain we have

$$(\widehat{\phi}_{\text{aux}}^p, \widehat{e}^{k,\{k_t\}})(T_k) = (\widehat{\phi}_{\text{aux}}^p, \widehat{e}^{k,\{k_t\}})(T_{k-1}) + \widehat{\mathcal{R}}^k(\widehat{U}^{k,\{k_t\}}, \widehat{\phi}_{\text{aux}}^p). \tag{36}$$

Summing from $k = 1$ to $k = p - 1$ and using (35),

$$(\phi^p - \widehat{\phi}, \widehat{e}^{p-1,\{k_t\}})(T_{p-1}) = \sum_{k=2}^{p-1} (\widehat{\phi}_{\text{aux}}^p, \widehat{U}^{k-1,\{k_t\}} - \widehat{U}^{k,\{k_t\}})(T_{k-1}) + \sum_{k=1}^{p-1} \widehat{\mathcal{R}}^k(\widehat{U}^{k,\{k_t\}}, \widehat{\phi}_{\text{aux}}^p) + (\widehat{\phi}_{\text{aux}}^p, \widehat{e}^{1,\{k_t\}})(0). \tag{37}$$

Combining (29) and (37) yields

$$\begin{aligned}
 (\psi, e^{\{k_t\}}(T)) &= \sum_{p=1}^{P_t} \mathcal{R}^p(U^{p,\{k_t\}}, \phi^p) + (\phi^1, \widehat{e}^{1,\{k_t\}})(0) \\
 &+ \sum_{p=2}^{P_t} \left[\sum_{k=2}^{p-1} (\widehat{\phi}_{\text{aux}}^p, \widehat{U}^{k-1,\{k_t\}} - \widehat{U}^{k,\{k_t\}})(T_{k-1}) + \sum_{k=1}^{p-1} \widehat{\mathcal{R}}^k(\widehat{U}^{k,\{k_t\}}, \widehat{\phi}_{\text{aux}}^p) + (\widehat{\phi}_{\text{aux}}^p, \widehat{e}^{1,\{k_t\}})(0) \right] \\
 &+ \sum_{p=2}^{P_t} \left[(\phi^p - \widehat{\phi}, \widehat{U}^{p-1,\{k_t\}} - U^{p,\{k_t\}}) + (\widehat{\phi}, U^{p-1,\{k_t\}} - U^{p,\{k_t\}}) \right] (T_{p-1}).
 \end{aligned} \tag{38}$$

We summarize as Theorem 1 below.

Theorem 1.

$$(\psi, e^{\{k_t\}}(T)) = \mathcal{D} + \mathcal{A} + \mathcal{C} + \mathcal{K}, \tag{39}$$

where

$$\begin{aligned}
\mathcal{D} &= \sum_{p=1}^{P_t} \mathcal{R}^p(U^{p,\{k_t\}}, \phi^p) + (\phi^1, \widehat{e}^{1,\{k_t\}})(0), \\
\mathcal{A} &= \sum_{p=2}^{P_t} \left[\sum_{k=2}^{p-1} (\widehat{\phi}_{\text{aux}}^p, \widehat{U}^{k-1,\{k_t\}} - \widehat{U}^{k,\{k_t\}})(T_{k-1}) + \sum_{k=1}^{p-1} \widehat{\mathcal{R}}^k(\widehat{U}^{k,\{k_t\}}, \widehat{\phi}_{\text{aux}}^p) + (\widehat{\phi}_{\text{aux}}^p, \widehat{e}^{1,\{k_t\}})(0) \right], \\
\mathcal{C} &= \sum_{p=2}^{P_t} (\phi^p - \widehat{\phi}, \widehat{U}^{p-1,\{k_t\}} - \widehat{U}^{p,\{k_t\}})(T_{p-1}), \\
\mathcal{K} &= \sum_{p=2}^{P_t} (\widehat{\phi}, U^{p-1,\{k_t\}} - U^{p,\{k_t\}})(T_{p-1}).
\end{aligned}$$

We identify the following components that comprise the total error.

1. \mathcal{D} is the “standard” fine scale discretization error contribution.
2. \mathcal{A} is the temporal auxiliary error contribution arising from the discontinuities in the fine scale adjoint solution at the synchronization points,
3. \mathcal{C} is the temporal coarse scale error contribution from the discontinuities in the coarse scale solution and the fine scale adjoint solution at synchronization points,
4. \mathcal{K} is the temporal iteration error contribution arising from the difference between the (fine scale) solutions at the synchronization points.

Numerical examples demonstrating the accuracy of this error estimator are provided in section 6.1. While the analysis above concerns the fine scale error, we note that the coarse scale error may also be estimated as described in C.

4.3 Extension to other time integrators

The analysis in the previous section assumed the implicit Euler method as the time integration procedure for both the coarse and fine scale solutions. However, the analysis remains valid provided the time integration method used at the fine and coarse scales satisfies (25) and (26). These requirements are satisfied for variational methods as demonstrated in §3. Moreover, these requirements are also satisfied for a number of numerical schemes which may be interpreted as a variational methods, e.g., Crank Nicolson, BDF, IMEX, etc [12, 11, 8, 9, 5].

5 *A posteriori* analysis of the Space-Time Parallel Algorithm (STPA)

In this section we derive error estimates for the error in the QoI computed from the fine scale solution of the STPA presented in §2.2. That is, we seek to estimate $\mathcal{Q}(u - U^{p,\{k_t, K_s\}}) = (\psi, u(T) - U^{p,\{k_t, K_s\}}(T))$. Theorem 1 also gives the error in the STPA by replacing by replacing $U^{p,\{k_t\}}$ with $U^{p,\{k_t, K_s\}}$. However, this result does not account for the error due to the spatial Schwarz domain decomposition iteration. In this section we extend the analysis to account for this source of error.

Let $U_n^{p,\{k_t, K_s\}} = U^{p,\{k_t, K_s\}}(t_n^p)$, where $U_n^{p,\{k_t, K_s\}}$ is the domain decomposition solution to (5) on time domain p for Parareal iteration k_t . More precisely, $U_n^{p,\{k_t, K_s\}}$ is the domain decomposition solution to the problem: find $U_n^{p,\{k_t\}} \in V_s^{q_s}$ such that

$$B^n(U_n^{p,\{k_t\}}, v) = l^n(v), \tag{40}$$

for all $v \in V_s^q$, where the bilinear form $B^n(\cdot, \cdot)$ and the linear form $l^n(\cdot)$ are given in (6), and $U_0^{p, \{k_t\}} = U_0^{p, \{k_t, K_s\}} = \widehat{U}^{p, \{k_t\}}(x, T_{p-1})$.

For analysis purposes we also introduce an analytical solution: find $u_n^{p, \{k_t\}} \in H_0^1(\Omega)$ such that,

$$B^n(u_n^{p, \{k_t\}}, v) = l^n(v) \quad \forall v \in H_0^1(\Omega). \quad (41)$$

Based on the discussion in section 3.3, we may also consider $u_n^{p, \{k_t\}}$ in variational form.

5.1 Overview of the strategy

Trivially,

$$\left(u(t_n^p) - U_n^{p, \{k_t, K_s\}}, \phi^p(t_n) \right) = \underbrace{\left(u(t_n^p) - u_n^{p, \{k_t\}}, \phi^p(t_n) \right)}_{\mathcal{E}_I} + \underbrace{\left(u_n^{p, \{k_t\}} - U_n^{p, \{k_t, K_s\}}, \phi^p(t_n) \right)}_{\mathcal{E}_{II}} \quad (42)$$

1. We estimate \mathcal{E}_I by interpreting $u_n^{p, \{k_t\}}$ as a variational solution and using *a posteriori* techniques developed in section 3.
2. We estimate \mathcal{E}_{II} using the *a posteriori* error analysis for overlapping domain decomposition presented in [4]. This analysis allows us to further split \mathcal{E}_{II} into iterative and discretization components.

5.2 Estimating \mathcal{E}_I

In a derivation akin to that of (18), interpreting $u_n^{p, \{k_t\}}$ as a space-time solution to the dG(0) method in time leads to,

$$\mathcal{E}_I = (\phi^p(t_n^p), u(t_n^p) - u_n^{p, \{k_t\}}) = (\phi^p(t_n^p), u(t_{n-1}^p) - U_{n-1}^{p, \{k_t, K_s\}}) + \mathcal{R}_n^p(u_n^{p, \{k_t\}}, \phi^p) \quad (43)$$

where we also used the fact that $u_n^{p, \{k_t\}}(t_{n-1}^p) = U_{n-1}^{p, \{k_t, K_s\}}$.

5.3 Estimating \mathcal{E}_{II}

The analysis of [4] is used to estimate the error term \mathcal{E}_{II} . We define the global (spatial) adjoint problem: find $\phi_n^p \in H_0^1(\Omega)$ such that,

$$B^n(v, \phi_n^p) = (\phi^p, v), \quad \forall v \in H_0^1(\Omega), \quad (44)$$

and adjoint problems on the spatial subdomains: find $\phi_{n,i}^{p, [k_s]} \in H_0^1(\Omega_i)$ such that,

$$B_i^n \left(v, \phi_{n,i}^{p, [k_s]} \right) = \tau \sum_{j=1}^{P_s} \left\{ (\phi^p(t_n)|_{\Omega_j}, v)_{ij} - B_{ij} \left(v, \sum_{l=k_s+1}^{K_s} \phi_{n,i}^{p, [l]} \right) \right\}, \quad \forall v \in H_0^1(\Omega_i), \quad (45)$$

where $\phi^p(t_n)|_{\Omega_i}$ is the restriction of $\phi^p(t_n)$ to Ω_i , and B_i^n and B_{ij}^n are the restrictions of B^n to Ω_i and Ω_{ij} respectively. For a fixed k_s , the adjoint problems (45) are independent for each i , so $\phi_{n,i}^{p, [k_s]}$ may be computed backwards from $K_s, K_s - 1, K_s - 2, \dots, 1$ in parallel analogous to the solution strategy in the additive Schwarz Algorithm 2.

Theorem 2.

$$\mathcal{E}_{II} = \left(u_n^{p, \{k_t\}} - U_n^{p, \{k_t, K_s\}}, \phi^p(t_n) \right) = \mathcal{D}_{k,n}^p + \mathcal{D}_{s,n}^p \quad (46)$$

where

$$\mathcal{D}_{s,n}^p = \sum_{i=1}^{P_s} \sum_{k_s=1}^{K_s} l^n(\phi_{n,i}^{p,[k_s]}) - B_i^n(\tilde{U}_{n,i}^{p,\{k_s\}}, \phi_{n,i}^{p,[k_s]}) \quad (47)$$

$$\mathcal{D}_{k,n}^p = l^n(\phi_n^p) - B^n(U_n^{p,\{k_t, K_s\}}, \phi_n^p) - \mathcal{D}_{s,n}^p \quad (48)$$

where $\tilde{U}_{n,i}^{p,\{k_s\}}$ are the spatial subdomain solutions on spatial subdomain i defined by (7).

The proof of Theorem 2 is provided in [4]. The term $\mathcal{D}_{s,n}^p$ quantifies the discretization error contribution (that is, due to using the spaces $V_{i,k_s}^{q_s}$) while the term $\mathcal{D}_{k,n}^p$ quantifies the domain decomposition iteration error contribution (that is, due to using a finite number K_s iterations).

5.4 Estimating $\mathcal{E}_I + \mathcal{E}_{II}$

Combining (43) and (46),

$$\begin{aligned} \mathcal{E}_I + \mathcal{E}_{II} &= (\phi^p(t_n^p), u(t_{n-1}^p) - U_{n-1}^{p,\{k_t, K_s\}}) + \mathcal{R}_n^p(U_n^{p,\{k_t, K_s\}}, \phi^p) \\ &= (\phi^p(t_n^p), u(t_{n-1}^p) - U_{n-1}^{p,\{k_t, K_s\}}) + \mathcal{R}_n^p(u_n^{p,\{k_t\}}, \phi^p) + \mathcal{D}_{k,n}^p + \mathcal{D}_{s,n}^p, \end{aligned} \quad (49)$$

To provide a comparison with the two part construction above, following the direct approach prescribed in (18) we have,

$$\mathcal{E}_I + \mathcal{E}_{II} = (\phi^p(t_n^p), u(t_n^p) - U_n^{p,\{k_t, K_s\}}) = (\phi^p(t_n^p), u(t_{n-1}^p) - U_{n-1}^{p,\{k_t, K_s\}}) + \mathcal{R}_n^p(U_n^{p,\{k_t, K_s\}}, \phi^p). \quad (50)$$

Comparing (50) and (49),

$$\mathcal{R}_n^p(U_n^{p,\{k_t, K_s\}}, \phi^p) = \mathcal{R}_n^p(u_n^{p,\{k_t\}}, \phi^p) + \mathcal{D}_{k,n}^p + \mathcal{D}_{s,n}^p. \quad (51)$$

Rearranging,

$$\mathcal{R}_n^p(u_n^{p,\{k_t\}}, \phi^p) = \mathcal{R}_n^p(U_n^{p,\{k_t, K_s\}}, \phi^p) - \mathcal{D}_{k,n}^p - \mathcal{D}_{s,n}^p. \quad (52)$$

Since all terms on the RHS of (52) are computable, so is $\mathcal{R}_n^p(u_n^{p,\{k_t\}}, \phi^p)$.

5.5 Summing contributions over time subdomain p

Using (22), the residual over the time domain $[T_{p-1}, T_p]$ is

$$\mathcal{R}^p(U_n^{p,\{k_t, K_s\}}, \phi^p) = \sum_{n=1}^{N_p} \mathcal{R}_n^p(U_n^{p,\{k_t, K_s\}}, \phi^p) = \sum_{n=1}^{N_p} \left(\mathcal{R}_n^p(u_n^{p,\{k_t\}}, \phi^p) + \mathcal{D}_{k,n}^p + \mathcal{D}_{s,n}^p \right) = \mathcal{D}_t^p + \mathcal{D}_s^p + \mathcal{D}_k^p \quad (53)$$

where

$$\mathcal{D}_t^p = \sum_{n=1}^{N_p} \mathcal{R}_n^p(u_n^{p,\{k_t\}}, \phi^p), \quad \mathcal{D}_k^p = \sum_{n=1}^{N_p} \mathcal{D}_{k,n}^p, \quad \mathcal{D}_s^p = \sum_{n=1}^{N_p} \mathcal{D}_{s,n}^p. \quad (54)$$

5.6 Error Representation for Space-Time Parallel Domain-Decomposition-Parareal Algorithm

Let $e^{\{k_t, K_s\}} = u(T) - U^{p,\{k_t, K_s\}}(T)$.

Theorem 3.

$$(\psi, e^{\{k_t, K_s\}}(T)) = \mathcal{D}_t + \mathcal{D}_s + \mathcal{D}_k + \mathcal{A} + \mathcal{C} + \mathcal{K}, \quad (55)$$

where \mathcal{A}, \mathcal{C} and \mathcal{K} are defined in Theorem 1 by (40) and,

$$\mathcal{D}_t = \sum_{p=1}^{P_t} \mathcal{D}_t^p + (\phi^1, \widehat{e}^{1, \{k_t\}})(0), \quad \mathcal{D}_s = \sum_{p=1}^{P_t} \mathcal{D}_s^p, \quad \mathcal{D}_k = \sum_{p=1}^{P_t} \mathcal{D}_k^p. \quad (56)$$

Proof. The proof follows directly from Theorem 1 by replacing $U^{p, \{k_t\}}$ with $U^{p, \{k_t, K_s\}}$ and then using (53). \square

We identify the following additional error components.

1. \mathcal{D}_t is the error contribution due to the use of implicit Euler time integration.
2. \mathcal{D}_s is the error contribution due to using a finite dimensional space for the solution of domain decomposition.
3. \mathcal{D}_k is the error contribution due to using a finite number, K_s , iterations of domain decomposition.

6 Numerical results

We present numerical results to support the analyses of both section 4 and section 5, highlighting the accuracy of the error estimates developed. Accordingly, we first consider the error analysis for the Time Parallel Algorithm of section 6.1 and then consider the effect of a further spatial domain decomposition iteration in the Space-Time Parallel Algorithm of section 6.2. The implicit Euler method is used in the fine and coarse scale solvers for these two sections. In section 6.3 we demonstrate the accuracy of the error estimates when a different time integration, a cG method, is employed in the coarse and fine scale solvers.

The accuracy of the *a posteriori* error estimates is measured by the effectivity ratio γ , where

$$\gamma = \frac{\text{Estimated error}}{\text{True error}}. \quad (57)$$

The bilinear and linear forms considered in the numerical examples are

$$a(u, v) = -(\nabla u, \nabla v) \quad \text{and} \quad l(v) = (f(x), v) \quad (58)$$

where

$$f(x) = \sin(\mu\pi x)(\mu^2\pi^2 \cos(\nu\pi t) - \nu\pi \sin(\nu\pi t)). \quad (59)$$

This choice of $f(x)$ corresponds to the true solution $u(x, t) = \cos(\nu\pi t) \sin(\mu\pi x)$. In all examples, the final time $T = 2$ and the quantity of interest at the final time T is defined by the ‘‘adjoint data’’

$$\psi(x) = \begin{cases} 10000[(x - 0.2)^2(x - 0.6)^2], & 0.2 < x < 0.6, \\ 0, & \text{otherwise.} \end{cases} \quad (60)$$

This choice of $\psi(x)$ corresponds to a local weighted average of the solution around $x = 0.4$ at the final time. The ratio of number of fine and coarse time steps is denoted by $r = N_t/\widehat{N}_t$. For the spatial discretization, the number of spatial finite elements at the two scales remained fixed, i.e., $N_s = \widehat{N}_s$, but different degrees of interpolation were employed according to whether the corresponding temporal integration was performed on the coarse or fine scales. A lower degree of spatial interpolation, \widehat{q}_s , was employed when constructing the solution on the coarse scale, and a higher degree of spatial interpolation,

q_s , was employed on the same spatial mesh when constructing the solution at the fine scale, i.e., $\hat{q}_s < q_s$. The notation used in this section is also summarized in A.

Two different time steps were employed for the temporal integration, a coarse time step and a smaller, fine time step. The implicit Euler method was chosen as the time integrator for the coarse and fine scale solvers \widehat{G} and F^p in §6.1 and §6.2. A continuous Galerkin method was used to obtain the results in §6.3. The adjoint solutions in (27), (28), (35), (44) and (45) need to be approximated. In all cases, the same temporal and spatial meshes were used as those used to compute the numerical solutions, however, higher degree approximations were employed to obtain accurate estimates. The adjoint solutions corresponding to (27), (28) and (35) were approximated on the space-time slab S_n^p using the cG(3) method in the space $W_{p,n}^{3,3}$ (see (9) for the definition of this space). The adjoint solutions (44) and (45), needed for the analysis of STPA, were approximated by using a spatial finite element employing continuous piecewise cubic polynomial functions.

6.1 Paralellism in time only: Time Parallel Algorithm

We first consider the *a posteriori* error estimate given by Theorem 1, Eq. (40) in section 4. The Parareal algorithm presents numerous discretization choices. We investigate the effect of the number of Parareal iterations in section 6.1.1, and the effect of the number of temporal subdomains in section 6.1.2. We then consider the effect of the fine time scale and the coarse time scale in sections 6.1.3 and 6.1.4 respectively. In sections 6.1.1 to 6.1.4, we ensure the temporal errors dominate spatial errors by choosing a modestly large number of spatial elements, so that the effects of changes to the spatial discretization parameters can be observed. Finally we consider the effect of the spatial discretization in section 6.1.5. In all cases the effectivity ratio of the error estimator is 1.00. For these examples $\nu = 4, \mu = 1$ in the function $f(x)$ in equation (59).

The examples not only provide convincing evidence of the accuracy of the error estimator, but illustrate the importance of identifying and estimating distinct error contributions. We observe fortuitous cancellation in the first example so that further refinement actually increases the error. The second example demonstrates a situation in which the refinement strategy has no effect on the overall error since it does not address the dominant source of error. Later examples show that when the dominant error term is targeted and it is at least an order of magnitude larger than all the other error contributions, refinements strategies have the anticipated effect on the overall error.

6.1.1 Effect of the number of Parareal iterations

The total error in Table 1 initially decreases with the number of Parareal iterations (K_t), but then increases somewhat. The initial decrease is expected, since for $K_t = 1$, the iteration error \mathcal{K} is the dominant source of error, and hence increasing the number of iterations leads to a decrease in this iteration error, and hence the overall error as well. However, after a single Parareal iteration, the iteration error \mathcal{K} is no longer the dominant error component. Rather the discretization error \mathcal{D} , which remains essentially constant during the iterative process, becomes the dominant error. Moreover, the discretization and iteration errors have opposite signs, and there is a fortuitous cancellation of error for $K_t = 2$ between these two terms. When the number of iterations is increased to 3, \mathcal{K} decreases as expected, but so does the cancellation of error between this term and \mathcal{D} , and hence the total error shows a modest increase.

K_t	Est. Err.	γ	\mathcal{D}	\mathcal{K}	\mathcal{C}	\mathcal{A}
1	-1.02e-01	1.00e+00	5.10e-02	-1.53e-01	0.00e+00	-2.30e-06
2	4.39e-02	1.00e+00	5.82e-02	-1.43e-02	2.86e-06	-2.91e-06
3	5.73e-02	1.00e+00	5.89e-02	-1.59e-03	3.11e-06	-2.96e-06

Table 1: $\widehat{N}_t = 20, r = 16, P_t = 10, \widehat{N}_s = 20, \widehat{q}_s = 1, q_s = 2$

6.1.2 Effect of the number of temporal subdomains

Increasing the number of temporal subdomains (P_t) is not expected to affect the discretization error \mathcal{D} which is determined by the spatial and temporal element scales, but is expected to increase the iteration error \mathcal{K} . Both are supported by the results in Table 2 below. The discretization error remains the largest error for all choices of the number of temporal subdomains.

P_t	Est. Err.	γ	\mathcal{D}	\mathcal{K}	\mathcal{C}	\mathcal{A}
2	1.16e-01	1.00e+00	1.16e-01	3.53e-07	-5.81e-09	-3.58e-08
5	1.16e-01	1.00e+00	1.16e-01	3.68e-05	6.18e-09	1.02e-07
10	1.12e-01	1.00e+00	1.15e-01	-3.26e-03	1.52e-08	9.56e-08

Table 2: $\widehat{N}_t = 40, r = 4, K_t = 2, \widehat{N}_s = 20, \widehat{q}_s = 1, q_s = 2$

6.1.3 Effect of the fine time scale

As is evident in Table 3, increasing the ratio r between the temporal fine and coarse scales reduces the discretization error \mathcal{D} . Since this is the dominant error, this also leads to a decrease in the total error.

r	Est. Err.	γ	\mathcal{D}	\mathcal{K}	\mathcal{C}	\mathcal{A}
2	7.21e-01	1.00e+00	7.31e-01	-9.49e-03	1.78e-04	-3.77e-04
4	3.82e-01	1.00e+00	4.06e-01	-2.31e-02	2.75e-04	-4.08e-04

Table 3: $\widehat{N}_t = 10, P_t = 10, K_t = 2, \widehat{q}_t = 1, q_t = 1, \widehat{N}_s = 20, \widehat{q}_s = 1, q_s = 2$

6.1.4 Effect of the coarse time scale

The results in Table 4 demonstrate that improving the accuracy of the coarse temporal solution reduces *all* components of the error, provided that the temporal errors dominate the spatial errors.

\widehat{N}_t	Est. Err.	γ	\mathcal{D}	\mathcal{K}	\mathcal{C}	\mathcal{A}
10	7.21e-01	1.00e+00	7.31e-01	-9.49e-03	1.78e-04	-3.77e-04
20	4.09e-01	1.00e+00	4.13e-01	-3.91e-03	1.42e-06	-2.94e-06

Table 4: $r = 2, P_t = 10, K_t = 2, \widehat{N}_s = 20, \widehat{q}_s = 1, q_s = 2$

6.1.5 Effect of the spatial scale

For the numerical results presented in Table 5 we have increased the number of coarse temporal elements to 100, r to 8, and the number of Parareal iterations to 6, in order to ensure the temporal errors are small compared with the spatial errors. While decreasing the discretization error as anticipated, improving the spatial accuracy is also seen to decrease the coarse temporal and auxiliary errors (though not monotonically) since these both have a spatial component.

\widehat{N}_s	Est. Err.	γ	\mathcal{D}	\mathcal{K}	\mathcal{C}	\mathcal{A}
5	6.61e-02	1.00e+00	6.61e-02	1.00e-10	1.16e-07	9.08e-07
10	3.40e-02	1.00e+00	3.40e-02	9.78e-11	2.20e-07	1.92e-06
20	2.64e-02	1.00e+00	2.64e-02	9.72e-11	2.51e-09	6.32e-08

Table 5: $\widehat{N}_t = 100, r = 8, P_t = 10, K_t = 6, \widehat{q}_s = 1, q_s = 1$

6.2 Space-Time Parallel Algorithm

The following results were obtained through a combination of the Parareal integration in time and additive Schwarz domain decomposition in space. We decompose the error \mathcal{D} in to its various components as presented in Theorem 3. The effects of varying the fine and coarse time scales are considered in sections 6.2.1 and 6.2.2 respectively. The number of domain decomposition iterations is varied in section 6.2.3, the number of spatial subdomains in section 6.2.4, and the degree of overlap of the spatial subdomains in 6.2.5. In all examples the effectivity ratio of the error estimator is 1.00. For these examples, we set $\nu = 4, \mu = 2$ in the function $f(x)$ defined by equation (59). The Richardson parameter used in spatial domain decomposition iterations was always set to $\tau = 0.4$.

Once again the examples not only provide convincing evidence of the accuracy of the error estimator, but illustrate the complex interplay that can occur between different contributions to the overall error. We frequently observe second order effects of a refinement strategy on error components other than those the strategy is directly targeting. These second order effects are largely inconsequential if the contributions to the overall error have widely different magnitude, but may become important when the error components are similar in scale and particularly when they are opposite in sign.

6.2.1 Effect of the fine time scale

Consistent with the results in §6.1.3, decreasing the temporal time step decreases the temporal component \mathcal{D}_t of the discretization error. Notice that for this example the number of spatial elements has been increased so that the temporal discretization error is dominant. All other error contributions in Table 6 are largely unaffected.

r	Est. Err.	γ	\mathcal{D}_t	\mathcal{D}_s	\mathcal{D}_k	\mathcal{K}	\mathcal{C}	\mathcal{A}
2	2.42e-01	1.00e+00	2.45e-01	6.94e-08	1.11e-02	7.98e-04	1.23e-02	-2.58e-02
4	1.55e-01	1.00e+00	1.48e-01	6.93e-08	1.37e-02	1.70e-03	1.95e-02	-2.65e-02
8	1.05e-01	1.00e+00	8.34e-02	7.32e-08	2.51e-02	2.12e-03	2.30e-02	-2.68e-02

Table 6: $\widehat{N}_t = 10, P_t = 10, K_t = 2, \widehat{N}_s = 80, P_s = 2, K_s = 8, \beta = 0.2, \widehat{q}_s = 1, q_s = 2$

6.2.2 Effect of the coarse time scale

Again, consistent with the results in section 6.1.4, all temporal components of the error decrease as the coarse time scale is decreased. The spatial error components in Table 7 are seen to be largely unaffected since the number of spatial elements has been chosen so that temporal errors dominate.

\widehat{N}_t	Est. Err.	γ	\mathcal{D}_t	\mathcal{D}_s	\mathcal{D}_k	\mathcal{K}	\mathcal{C}	\mathcal{A}
10	2.42e-01	1.00e+00	2.45e-01	6.94e-08	1.11e-02	7.98e-04	1.23e-02	-2.58e-02
20	1.55e-01	1.00e+00	1.41e-01	6.55e-08	1.46e-02	-9.88e-07	-5.09e-04	-4.81e-05
40	1.05e-01	1.00e+00	7.95e-02	6.89e-08	2.54e-02	-4.12e-07	-8.73e-06	-3.05e-07

 Table 7: $r = 2$, $P_t = 10$, $K_t = 2$, $\widehat{N}_s = 80$, $P_s = 2$, $K_s=8$, $\beta = 0.2$, $\widehat{q}_s = 1$, $q_s = 2$

6.2.3 Effect of the number of domain decomposition iterations

The spatial iteration error \mathcal{D}_k decreases with number of domain decomposition iterations, as shown in Table 8, while the spatial and temporal discretization errors remain essentially constant. There is a second order effect of decreasing the temporal iterative and coarse time scale error contributions since these error contributions also have a spatial component.

K_s	Est. Err.	γ	\mathcal{D}_t	\mathcal{D}_s	\mathcal{D}_k	\mathcal{K}	\mathcal{C}	\mathcal{A}
2	6.61e-01	1.00e+00	2.16e-01	1.95e-05	4.49e-01	-1.10e-04	-4.94e-03	-4.52e-05
6	1.88e-01	1.00e+00	1.45e-01	1.71e-05	4.40e-02	-1.84e-05	-1.31e-03	-4.87e-05

 Table 8: $\widehat{N}_t = 20$, $r = 2$, $P_t = 10$, $K_t = 2$, $\widehat{N}_s = 20$, $P_s = 2$, $\beta = 0.2$, $\widehat{q}_s = 1$, $q_s = 2$

6.2.4 Effect of the number of spatial subdomains

The spatial iteration error \mathcal{D}_k increases with number of spatial subdomains, while the spatial and temporal discretization errors remain essentially constant. A second order effect is again apparent in Table 9, where the temporal iterative error is seen to also increase due to its spatial component.

P_s	Est. Err.	γ	\mathcal{D}_t	\mathcal{D}_s	\mathcal{D}_k	\mathcal{K}	\mathcal{C}	\mathcal{A}
2	7.17e-01	1.00e+00	2.25e-01	1.02e-06	4.96e-01	-8.83e-06	-4.51e-03	-4.46e-05
4	1.23e+00	1.00e+00	3.13e-01	1.26e-06	9.18e-01	3.84e-05	-5.76e-03	-4.43e-05

 Table 9: $\widehat{N}_t = 20$, $r = 2$, $P_t = 10$, $K_t = 2$, $\widehat{N}_s = 40$, $K_s=2$, $\beta = 0.1$, $\widehat{q}_s = 1$, $q_s = 2$

6.2.5 Effect of spatial domain overlap

Increasing the degree of overlap between the spatial domains is expected to decrease the spatial iterative error \mathcal{D}_k while leaving the spatial and temporal discretization errors largely unchanged. Slightly different behavior is observed in Table 10 for this example, perhaps because the temporal discretization error is orders of magnitude larger than the spatial discretization error. Never-the-less, the error estimator is accurate and the effectivity ratio is 1.00.

β	Est. Err.	γ	\mathcal{D}_t	\mathcal{D}_s	\mathcal{D}_k	\mathcal{K}	\mathcal{C}	\mathcal{A}
0.1	7.17e-01	1.00e+00	2.25e-01	1.02e-06	4.96e-01	-8.83e-06	-4.51e-03	-4.46e-05
0.2	6.61e-01	1.00e+00	2.16e-01	1.95e-05	4.49e-01	-1.10e-04	-4.94e-03	-4.52e-05

 Table 10: $\widehat{N}_t = 20$, $r = 2$, $P_t = 10$, $K_t = 2$, $\widehat{N}_s = 20$, $P_s = 2$, $K_s=2$, $\widehat{q}_s = 1$, $q_s = 2$

6.3 Results for a different time integrator for the Time parallel Algorithm

We briefly demonstrate the accuracy of the *a posteriori* error estimates when the continuous Galerkin method, $cG(q_t)$ (see section 3), is employed as the time integration scheme in the fine and coarse scale solvers for the TPA. The approximation space for the coarse and fine scales on the the space-time slab S_h^p are $W_{p,n}^{\hat{q}_t, \hat{q}_s}$ and $W_{p,n}^{q_t, q_s}$ respectively. The results of Theorems 1 and 3 remain valid; however, the definition of the residuals involved need to be modified to reflect the cG method. The residual for the cG method is given in (14). The results are qualitative similar to those in section 6.1, and hence we present them without any comment. The aim is to show that the results are still accurate, and that the analysis is applicable to a broad class of numerical methods. The results are given in Tables 11, 12, 13, 14 and 15.

K_t	Est. Err.	γ	\mathcal{D}	\mathcal{K}	\mathcal{C}	\mathcal{A}
1	1.02e-01	1.00e+00	-4.46e-02	1.47e-01	0.00e+00	1.79e-04
2	-6.34e-02	1.00e+00	-3.86e-02	-2.48e-02	-1.99e-04	1.80e-04
3	-3.81e-02	1.00e+00	-3.96e-02	1.50e-03	-1.67e-04	1.80e-04

Table 11: $\hat{N}_t = 10$, $r = 4$, $P_t = 10$, $\hat{q}_t = 1$, $q_t = 1$, $\hat{N}_s = 20$, $\hat{q}_s = 1$, $q_s = 2$

P_t	Est. Err.	γ	\mathcal{D}	\mathcal{K}	\mathcal{C}	\mathcal{A}
2	-3.95e-02	1.00e+00	-3.95e-02	3.86e-07	1.28e-07	1.20e-08
5	-3.96e-02	1.00e+00	-3.95e-02	-2.55e-05	6.94e-05	-7.27e-05
10	-6.34e-02	1.00e+00	-3.86e-02	-2.48e-02	-1.99e-04	1.80e-04

Table 12: $\hat{N}_t = 10$, $r = 4$, $K_t = 2$, $\hat{q}_t = 1$, $q_t = 1$, $\hat{N}_s = 20$, $\hat{q}_s = 1$, $q_s = 2$

r	Est. Err.	γ	\mathcal{D}	\mathcal{K}	\mathcal{C}	\mathcal{A}
2	-1.71e-01	1.00e+00	-1.53e-01	-1.82e-02	-1.57e-04	1.78e-04
4	-6.34e-02	1.00e+00	-3.86e-02	-2.48e-02	-1.99e-04	1.80e-04

Table 13: $\hat{N}_t = 10$, $P_t = 10$, $K_t = 2$, $\hat{q}_t = 1$, $q_t = 1$, $\hat{N}_s = 20$, $\hat{q}_s = 1$, $q_s = 2$

\hat{N}_t	Est. Err.	γ	\mathcal{D}	\mathcal{K}	\mathcal{C}	\mathcal{A}
10	-1.71e-01	1.00e+00	-1.53e-01	-1.82e-02	-1.57e-04	1.78e-04
20	-4.10e-02	1.00e+00	-3.95e-02	-1.55e-03	-5.17e-07	6.50e-07

Table 14: $r = 2$, $P_t = 10$, $K_t = 2$, $\hat{q}_t = 1$, $q_t = 1$, $\hat{N}_s = 20$, $\hat{q}_s = 1$, $q_s = 2$

\hat{N}_s	Est. Err.	γ	\mathcal{D}	\mathcal{K}	\mathcal{C}	\mathcal{A}
5	3.73e-02	1.00e+00	3.69e-02	1.68e-10	-1.95e-05	8.85e-04
10	5.55e-03	1.00e+00	5.54e-03	1.40e-10	-7.21e-07	4.15e-05
20	-1.93e-03	1.00e+00	-1.93e-03	1.33e-10	-6.45e-07	2.55e-07

Table 15: $\hat{N}_t = 20$, $r = 6$, $P_t = 10$, $K_t = 6$, $\hat{q}_t = 1$, $q_t = 1$, $\hat{q}_s = 1$, $q_s = 1$

7 Conclusions and future work

We first developed an accurate adjoint-based *a posteriori error* analysis for the Time Parallel Algorithm, which applies the Parareal method in time for the solution of parabolic partial differential equations. This analysis does not seek to separate spatial and temporal sources of error, but combines the two as “discretization” error. Additional error contributions arise due to incomplete iteration, discontinuities in the coarse forward solution, and the fine adjoint solution when it is solved in parallel. We then extended this analysis to the Space-Time Parallel Algorithm by assuming that the spatial solution is determined through a second iterative method, in this case domain decomposition. The combined analysis is able to disaggregate the spatial and temporal discretization errors, as well as identify additional iterative errors resulting from the domain decomposition iteration in space. Thus the analysis presented here provides a basis for separating discretization and iteration errors and for estimating the effects of incomplete iteration in both space and time. Accurate error estimates provide a foundation for adaptivity and are essential for accurate uncertainty quantification where it is necessary to distinguish variation due to parameter changes from variation due to numerical errors which can also vary across the parameter domain.

We have limited the analysis to linear problems and intend to extend these results to nonlinear problems using linearization techniques that have previously proven effective [7]. We also investigate more sophisticated temporal solvers than backward Euler and a simple cG method. Parallel iterative methods for solving PDEs require a large number of discretization choices. The error analysis developed here, which accurately distinguishes multiple sources of error, provides a sound foundation on which to make many of these choices. Finally, we can investigate adaptive strategies, noting the complex interaction between error components.

Waveform relaxation methods [23, 24, 25] make a fundamentally different choice when combining the two iterative methods of domain decomposition and Parareal iteration. Assume we wish to solve a parabolic partial differential equation on $\Omega \times (0, T]$ and let $\Omega_i \subset \Omega, i = 1, \dots, p$ be a set of overlapping (spatial) subdomains. Waveform relaxation methods consider domain decomposition as the outer iteration and employs Parareal iteration (or some other time integration technique) to solve subproblems on each spatio-temporal subdomain $\Omega_i \times (0, T], i = 1, \dots, p$ independently, and then perform a domain decomposition like iteration on the p spatial-temporal blocks. Efficient implementations of waveform relaxation require additional computation to determine Robin conditions for the boundaries of subdomains. An analysis of this approach is saved for future work, starting with an *a posteriori error* analysis for waveform relaxation implementing a simple, discontinuous Galerkin method for time integration and then extending to Parareal integration in time.

Acknowledgments

J. Chaudhry’s work is supported by the NSF-DMS 1720402. S. Tavener’s work is supported by NSF-DMS 1720473. D. Estep’s work is supported by NSF-DMS 1720473 and NSERC grants.

References

- [1] M. Ainsworth and T. Oden. *A posteriori error estimation in finite element analysis*. John Wiley-Teubner, 2000.
- [2] R. Becker and R. Rannacher. An optimal control approach to *a posteriori error* estimation in finite element methods. *Acta Numerica*, pages 1–102, 2001.
- [3] Tony F Chan and Tarek P Mathew. Domain decomposition algorithms. *Acta numerica*, 3:61–143, 1994.

- [4] Jehanzeb Chaudhry, Don Estep, and Simon Tavener. A posteriori error analysis for schwarz overlapping domain decomposition methods. *arXiv preprint arXiv:1907.01139*, 2019.
- [5] Jehanzeb H Chaudhry and JB Collins. A posteriori error estimation for the spectral deferred correction method. *arXiv preprint arXiv:2003.03399*, 2020.
- [6] Jehanzeb H. Chaudhry, Donald Estep, , Victor Ginting, and Simon Tavener. A posteriori analysis of an iterative multi-discretization method for reaction-diffusion systems. *Computer Methods in Applied Mechanics and Engineering*, 267(0):1 – 22, 2013.
- [7] Jehanzeb Hameed Chaudhry, Don Estep, Simon Tavener, Varis Carey, and Jeff Sandelin. A posteriori error analysis of two-stage computation methods with application to efficient discretization and the parareal algorithm. *SIAM Journal on Numerical Analysis*, 54(5):2974–3002, 2016.
- [8] J.H. Chaudhry, D. Estep, V. Ginting, J.N. Shadid, and S.J. Tavener. A posteriori error analysis of IMEX multi-step time integration methods for advection–diffusion–reaction equations. *Computer Methods in Applied Mechanics and Engineering*, 285:730–751, Mar 2015.
- [9] J.H. Chaudhry, J.N. Shadid, and T. Wildey. A posteriori analysis of an IMEX entropy-viscosity formulation for hyperbolic conservation laws with dissipation. *Applied Numerical Mathematics*, 135, 2019.
- [10] J. H. Chaudry, D. Estep, V. Ginting, and S. Tavener. A posteriori analysis for iterative solvers for non-autonomous evolution problems. *SIAM Journal on Uncertainty Quantification*, 3, 2015.
- [11] J. Collins, D. Estep, and S.J. Tavener. A posteriori error estimates for explicit time integration methods. *BIT Numerical Mathematics*, 2014.
- [12] J.B. Collins, D. Estep, and S.J. Tavener. A posteriori error estimation for the Lax–Wendroff finite difference scheme. *Journal of Computational and Applied Mathematics*, 263:299–311, 2014.
- [13] Victorita Dolean, Pierre Jolivet, and Frédéric Nataf. *An introduction to domain decomposition methods: algorithms, theory, and parallel implementation*. SIAM, 2015.
- [14] Matthew Emmett and Michael Minion. Toward an efficient parallel in time method for partial differential equations. *Communications in Applied Mathematics and Computational Science*, 7(1):105–132, 2012.
- [15] Matthew Emmett and Michael L Minion. Efficient implementation of a multi-level parallel in time algorithm. In *Domain Decomposition Methods in Science and Engineering XXI*, pages 359–366. Springer, 2014.
- [16] K. Eriksson, D. Estep, P. Hansbo, and C. Johnson. *Computational Differential Equations*. Cambridge University Press, Cambridge, 1996.
- [17] Kenneth Eriksson, Don Estep, Peter Hansbo, and Claes Johnson. Introduction to adaptive methods for differential equations. *Acta numerica*, 4:105–158, 1995.
- [18] D Estep, V Ginting, and S Tavener. A posteriori analysis of a multirate numerical method for ordinary differential equations. *Computer Methods in Applied Mechanics and Engineering*, 223:10–27, 2012.
- [19] Robert D Falgout, Stephanie Friedhoff, Tz V Kolev, Scott P MacLachlan, and Jacob B Schroder. Parallel time integration with multigrid. *SIAM Journal on Scientific Computing*, 36(6):C635–C661, 2014.

- [20] Robert D Falgout, Stephanie Friedhoff, Tz V Kolev, Scott P MacLachlan, Jacob B Schroder, and Stefan Vandewalle. Multigrid methods with space–time concurrency. *Computing and Visualization in Science*, 18(4):123–143, 2017.
- [21] M. Gander and S. Vandewalle. Analysis of the parareal time-parallel time-integration method. *SIAM Journal on Scientific Computing*, 29(2):556–578, 2007.
- [22] Martin J Gander. 50 years of time parallel time integration. In *Multiple shooting and time domain decomposition methods*, pages 69–113. Springer, 2015.
- [23] Martin J Gander and Laurence Halpern. Optimized schwarz waveform relaxation methods for advection reaction diffusion problems. *SIAM Journal on Numerical Analysis*, 45(2):666–697, 2007.
- [24] Martin J Gander, Yao-Lin Jiang, and Rong-Jian Li. Parareal schwarz waveform relaxation methods. In *Domain Decomposition Methods in Science and Engineering XX*, pages 451–458. Springer, 2013.
- [25] Martin J Gander and Andrew M Stuart. Space-time continuous analysis of waveform relaxation for the heat equation. *SIAM Journal on Scientific Computing*, 19(6):2014–2031, 1998.
- [26] MartinJ. Gander and Ernst Hairer. Nonlinear convergence analysis for the parareal algorithm. In *Domain Decomposition Methods in Science and Engineering XVII*, volume 60 of *Lecture Notes in Computational Science and Engineering*, pages 45–56. Springer Berlin Heidelberg, 2008.
- [27] M.B. Giles and E. Süli. Adjoint methods for pdes: a posteriori error analysis and postprocessing by duality. *Acta Numerica*, 11(1):145–236, 2002.
- [28] SEBASTIAN Gotschel and Michael L Minion. An efficient parallel-in-time method for optimization with parabolic pdes. *SIAM Journal on Scientific Computing*, 41(6):C603–C626, 2019.
- [29] Alexander J Howse, Hans De Sterck, Robert D Falgout, Scott MacLachlan, and Jacob Schroder. Parallel-in-time multigrid with adaptive spatial coarsening for the linear advection and inviscid burgers equations. *SIAM Journal on Scientific Computing*, 41(1):A538–A565, 2019.
- [30] David E. Keyes, Youcef Saad, and Donald G. Truhlar, editors. *Domain-Based Parallelism and Problem Decomposition Methods in Computational Sciences and Engineering*. SIAM, 1995.
- [31] C. Evans Lawrence. *Partial Differential Equations*, volume 19 of *Graduate Studies in Mathematics*. AMS, 2010.
- [32] Pierre-Louis Lions. On the schwarz alternating method. iii: a variant for nonoverlapping subdomains. In *Third international symposium on domain decomposition methods for partial differential equations*, volume 6, pages 202–223. SIAM Philadelphia, PA, 1990.
- [33] Pierre-Louis Lions et al. On the schwarz alternating method. i. In *First international symposium on domain decomposition methods for partial differential equations*, volume 1, page 42. Paris, France, 1988.
- [34] Y. Maday. The parareal in time algorithm. 2008.
- [35] Yvon Maday and Gabriel Turinici. A parareal in time procedure for the control of partial differential equations. *Comptes Rendus Mathematique*, 335(4):387–392, 2002.
- [36] Yvon Maday and Gabriel Turinici. A parareal in time procedure for the control of partial differential equations. *Comptes Rendus Mathematique*, 335(4):387–392, 2002.

- [37] Tarek Poonithara Abraham Mathew. *Domain Decomposition Methods for the Numerical Solution of Partial Differential Equations*, volume 61 of *Lecture Notes in Computational Science and Engineering*. Springer Berlin Heidelberg, Berlin, Heidelberg, 2008.
- [38] Benjamin W Ong and Jacob B Schroder. Applications of time parallelization. *Computing and Visualization in Science*, 23(1):1–15, 2020.
- [39] Barry F. Smith, Petter E. Bjørstad, and William Gropp. *Domain Decomposition: Parallel Multilevel Methods for Elliptic Partial Differential Equations*. Cambridge University Press, 1996.
- [40] Andrea Toselli and Olof Widlund. *Domain Decomposition Methods - Algorithms and Theory*, volume 34 of *Springer Series in Computational Mathematics*. Springer, 2004.
- [41] Jinchao Xu. Iterative methods by space decomposition and subspace correction. *SIAM review*, 34(4):581–613, 1992.

A Notation

Variables, errors and residuals

	Solutions
u	Analytic solution
U^p	Fine scale discrete solution on the p th temporal subdomain
\widehat{U}^p	Coarse scale discrete solution on the p th temporal subdomain
$U^{p,\{k_t\}}$	Fine scale discrete solution on the p th temporal subdomain after k_t parareal iterations
$U^{p,\{k_t,k_s\}}$	Fine scale discrete solution on the p th temporal subdomain after k_t parareal iterations and k_s domain decomposition iterations
	Errors and residuals
e^p	Fine scale error on the p th temporal subdomain
\widehat{e}^p	Coarse scale error on the p th temporal subdomain
\mathcal{R}^p	Fine scale residual on the p th temporal subdomain
$\widehat{\mathcal{R}}^p$	Coarse scale residual on the p th temporal subdomain
$\widehat{\mathcal{R}}_{\text{aux}}^p$	Auxiliary adjoint problem residual on the p th temporal subdomain
	Adjoints
ϕ	Fine scale adjoint solution
ϕ^p	Fine scale adjoint solution on the p th temporal subdomain
$\widehat{\phi}$	Coarse scale adjoint solution
$\widehat{\phi}_{\text{aux}}^p$	Auxiliary adjoint solution on the p th temporal subdomain

Table 16: Notation: Variables, errors and residuals

Discretization choices

Time	
N_t	Number of fine scale temporal finite elements
\widehat{N}_t	Number of coarse scale temporal finite elements
r	N_t/\widehat{N}_t . Refinement factor for time
q_t	Interpolation degree of fine scale temporal finite elements
\widehat{q}_t	Interpolation degree of coarse scale temporal finite elements
P_t	Number of parareal subdomains (synchronization intervals)
K_t	Number of parareal iterations
Space	
N_s	Number of fine scale spatial finite elements
\widehat{N}_s	Number of coarse scale spatial finite elements
q_s	Interpolation degree of fine scale spatial finite elements
\widehat{q}_s	Interpolation degree of coarse scale spatial finite elements
P_s	Number of spatial subdomains
K_s	Number of domain decomposition iterations
β	Amount of spatial overlap

Table 17: Notation: Discretization choices

Time discretization

T_{p-1}	Left hand end of p th time subdomain
T_p	Right hand end of p th time subdomain
Course scale solution	
\widehat{N}_t^p	Number of coarse scale temporal finite elements in p th time subdomain
\widehat{t}_{j-1}^p	Left hand end of j th coarse time interval in p th time subdomain
\widehat{t}_j^p	Right hand end of j th coarse time interval in p th time subdomain
$\widehat{\mathcal{I}}_j^p$	$[\widehat{t}_{j-1}^p, \widehat{t}_j^p]$
$\widehat{\mathcal{T}}^p$	$\{\widehat{\mathcal{I}}_1^p, \dots, \widehat{\mathcal{I}}_j^p, \dots, \widehat{\mathcal{I}}_{\widehat{N}_t^p}^p\}$
Fine scale solution	
N_t^p	Number of fine scale temporal finite elements in p th time subdomain
t_{j-1}^p	Left hand end of j th fine time interval in p th time subdomain
t_j^p	Right hand end of j th fine time interval in p th time subdomain
\mathcal{I}_j^p	$[t_{j-1}^p, t_j^p]$
\mathcal{T}^p	$\{\mathcal{I}_1^p, \dots, \mathcal{I}_j^p, \dots, \mathcal{I}_{N_t^p}^p\}$

Table 18: Notation: Time discretization

B Standard Parareal algorithm and equivalence

The standard Parareal algorithm only defines the solutions at the times T_p [34]. This algorithm is given in Algorithm 3 Here $\widetilde{U}_p^{(k_t)} \in V_s^{\widehat{q}_s}$ and $\overline{U}_p^{(k_t)} \in V_s^{q_s}$ are the coarse and fine scale solutions at T_p at iteration k_t .

Algorithm 3 Standard form of the Parareal algorithm

```

procedure PAR( $P_t, K_t, \widehat{U}_0$ )
   $C^{p,\{0\}} = 0, p = 0, \dots, P_t$  ▷ Initialize corrections
  for  $k_t = 1, \dots, K_t$  do
     $\widetilde{U}_0^{(k_t)} := \widehat{U}_0$  ▷ Set initial conditions
    for  $p = 1, \dots, P_t$  do
       $\widetilde{U}_p^{(k_t)} = \widehat{G}^p \left[ \widetilde{U}_{p-1}^{(k_t)} \right] (T_p) + C_p^{k_t-1}$  ▷ Serial computation
       $\overline{U}_p^{(k_t)} = F^p \left[ \widetilde{U}_{p-1}^{(k_t)} \right] (T_p)$  ▷ Parallel computation
       $C_p^{k_t} = \overline{U}_p^{(k_t)} - \widehat{G}^p \left[ \widetilde{U}_{p-1}^{(k_t)} \right] (T_p)$  ▷ Update corrections
    end for
  end for
end procedure

```

Theorem 4. *The standard Parareal algorithm in Algorithm 3 and the variational version in Algorithm 1 are equivalent in the sense that,*

$$\widetilde{U}_p^{(K_t)} = \widehat{U}^{p,\{K_t\}}(x, T_p) + C^{p,\{K_t-1\}} \quad (61)$$

$$\overline{U}_p^{(K_t)} = U^{p,\{K_t\}}(x, T_p) \quad (62)$$

$$C^{p,\{K_t\}} = C^{p,\{K_t\}} \quad (63)$$

For proof, please see [7].

C Coarse scale error

While the focus of the article is on the fine scale error, we briefly outline the result for the coarse scale error for completeness. Let $\widehat{e}^{p,\{k_t\}} = u - \widehat{U}^{p,\{k_t\}}$. Then,

Theorem 5.

$$(\psi_T, \widehat{e}^{P_t,\{k_t\}}(T)) = \sum_{p=1}^{P_t} \widehat{\mathcal{R}}^p(\widehat{U}^{p,\{k_t\}}, \widehat{\phi}) - \sum_{p=1}^{P_t-1} (\widehat{\phi}(T_p), C^{p,\{k_t-1\}}) + (\widehat{\phi}(0), \widehat{e}^{1,\{k_t\}}(0)). \quad (64)$$

The proof is similar to the proof of Theorem 1.